Limit on T-violating P-conserving ρNN interaction from the γ decay of ^{57}Fe

M. T. Ressell
W. K. Kellogg Radiation Laboratory, 106-38, California Institute of Technology, Pasadena, California 91125

J. Engel
Department of Physics and Astronomy, University of North Carolina, Chapel Hill, North Carolina 27599

P. Vogel
Department of Physics, 161-33, California Institute of Technology, Pasadena, California 91125
(Received 5 December 1995)

We use the experimental limit on the interference of $M1$ and $E2$ multipoles in the γ decay of ^{57}Fe to bound the time-reversal-violating parity-conserving ρNN vertex. Our approach is a large-basis shell-model calculation of the interference. We find an upper limit on the parameter $\overline{g_\rho}$, the relative strength of the T-violating ρNN vertex, of close to 10^{-2}, a value similar to the best limits from other experiments.

PACS number(s): 24.80.+y, 21.60.Cs, 21.30.Fe, 23.20.Gq

For many years it has been difficult to compare the quality of limits on time-reversal-violating parity-conserving (TVPC) interactions coming from different low-energy experiments. The experiments typically limit observables unique to themselves, and before comparisons can be made, these limits must be translated into a common TVPC quantity. It turns out that a convenient measure of nuclear TVPC interactions is the dimensionless ratio, often called $\overline{g_\rho}$ [1], of the TVPC ρ-meson–nucleon coupling to the normal strong coupling g_ρ. Among the other mesons only those with axial-vector couplings can transmit TVPC interactions between nucleons via a single exchange [2], and they are significantly heavier than the ρ and consequently less effective in nuclei. It is therefore reasonable to treat all TVPC nucleon-nucleon interactions as arising from ρ exchange, and to use $\overline{g_\rho}$ to parametrize their strength.

Experimental upper limits on several quantities, including the electric dipole moments of the neutron and of ^{199}Hg [1], and a correlation in the scattering of polarized neutrons from aligned ^{165}Ho [3], have been translated into limits on $\overline{g_\rho}$, constraining it to be less than about 10^{-2}. A number of other experiments, looking, e.g., for the violation of detailed balance [4], remain to be similarly interpreted. In this paper we report an examination of a 1977 experiment [5] that searched for interference between $M1$ and $E2$ radiation in the γ decay of the first $5/2^-$ state in ^{57}Fe to the first $3/2^-$ state. (Neither is the ground state; the two have excitation energies of 137 keV and 14 keV.) Our approach was to diagonalize the strong nuclear Hamiltonian in the shell model, and then treat the TVPC ρ-exchange interaction as a perturbation that causes the interference by mixing higher-lying states into the two involved in the transition. Reference [6] employed this method to constrain the TVPC coupling of the A_1 meson to the nucleon from the same experiment, but used what we argue is too small a model space. In addition, the lighter and more commonly considered ρ meson was neglected completely.

The $M1$-$E2$ interference that signals T violation can be expressed in terms of $\sin\eta$,[1] the imaginary part of the multipole mixing ratio δ, [7] which is defined as [8]

$$\delta=\frac{\langle J_f\|T^{M_1}\|J_i\rangle}{\langle J_f\|T^{E_2}\|J_i\rangle}=|\delta|(\cos\eta+i\,\sin\eta). \tag{1}$$

In Ref. [5] the upper limit on $|\sin\eta|$ was expressed in the form of a measured value that included zero within experimental accuracy:

$$|\sin\eta|=(3.1\pm 6.5)\times 10^{-4}. \tag{2}$$

The contributions to η can be written as

$$\eta=\varepsilon_{E2}-\varepsilon_{M1}+\xi, \quad \varepsilon_{E2},\varepsilon_{M1},\xi\ll 1, \tag{3}$$

where the last term ξ represents effects of final state interactions, which have been shown [9] to be smaller than the upper limit in Eq. (2).

In first-order perturbation theory, the difference between the two ε's is [10]

$$\begin{aligned} i(\varepsilon_{E2}-\varepsilon_{M1})=&\sum_n \frac{\langle J_f|V_\rho|nJ_f\rangle}{E_f-E_n}\left(\frac{\langle nJ_f\|E2\|J_i\rangle}{\langle J_f\|E2\|J_i\rangle}\right.\\ &\left.-\frac{\langle nJ_f\|M1\|J_i\rangle}{\langle J_f\|M1\|J_i\rangle}\right)\\ &+\sum_n \frac{\langle nJ_i|V_\rho|J_i\rangle}{E_i-E_n}\left(\frac{\langle J_f\|E2\|nJ_i\rangle}{\langle J_f\|E2\|J_i\rangle}\right.\\ &\left.-\frac{\langle J_f\|M1\|nJ_i\rangle}{\langle J_f\|M1\|J_i\rangle}\right). \end{aligned} \tag{4}$$

[1] $\sin\eta$ is directly proportional to the experimental correlation $(\mathbf{J}\cdot\mathbf{q}\times\mathbf{E})(\mathbf{J}\cdot\mathbf{q})(\mathbf{J}\cdot\mathbf{E})$, where $\mathbf{J}$ is the quantization axis of the initial nucleus, $\mathbf{E}$ is the photon electric field vector, and $\mathbf{q}$ is the photon direction [5].

With nucleons represented by i,j, the two-body ρ-exchange potential has the form

$$V^{\rho}=\sum_{i,j}\mathscr{V}^{\rho}_{i,j}[\tau_i\times\tau_j]_3,$$
$$\mathscr{V}^{\rho}_{i,j}=\frac{m_\rho^3 g_\rho^2\overline{g_\rho}\mu_v}{4\pi M^2}\frac{e^{-m_\rho r_{ij}}}{m_\rho^3 r_{ij}^3}(1+m_\rho r_{ij})(\boldsymbol{\sigma}_i-\boldsymbol{\sigma}_j)\cdot l, \tag{5}$$

where $\mathbf{r}_{ij}=\mathbf{r}_i-\mathbf{r}_j$, $l=\mathbf{r}_{ij}\times(1/2)(\mathbf{p}_i-\mathbf{p}_j)$, $\mu_v=3.70$ n.m. is the isovector nucleon magnetic moment, M is the nucleon mass, $g_\rho=2.79$ is the normal strong ρNN coupling, and $\overline{g_\rho}$ is the quantity that we are trying to constrain. After choosing a model space and interaction (and a reasonable prescription for treating short-range correlations [1,6]), we can use this formalism in a shell-model calculation to translate the experimental limit on $\sin\eta$ to a limit on $\overline{g_\rho}$.

The issues surrounding the calculation are more complicated than they initially appear, however. To evaluate the phases in Eq. (4) one needs, in principle, the wave functions and energies of *all* $3/2^-$ and $5/2^-$ states in ^{57}Fe. To obtain them, one ought to diagonalize the best available nuclear hamiltonian for 17 valence nucleons moving freely in the pf shell. Such a space has an m-scheme dimension of $\sim 4.5\times 10^8$. At the other extreme is a minimal model space, based on the well-established shell closure at N or $Z=28$, consisting of 3 valence neutrons in the $(2p_{3/2},1f_{5/2},2p_{1/2})$ shells and the remaining 14 nucleons in the $1f_{7/2}$ subshell. This ''small space'' is the one used in Ref. [6] and contains few enough states to allow direct diagonalization of any Hamiltonian. Unfortunately this space artificially restricts the $M1$ strength from any given state because it does not allow the important $1f_{7/2}$-$1f_{5/2}$ spin-flip transition. Consequently, in the calculations described here we used a ''large space,'' constructed by allowing a single proton or neutron to move out of the $1f_{7/2}$ shell into any one of the other subshells. The large space contains 23604 m-scheme states, forcing an approximate diagonalization.

To obtain the approximate wave functions we used the Lanczos algorithm as implemented in the shell-model code CRUNCHER [11] and its auxiliary codes, with slight modifications to accommodate the imaginary two-body matrix elements of the interaction in Eq. (5). Since it was not practical to calculate all $J^\pi=3/2^-$ and $5/2^-$ wave functions (there are 2052 and 2755 of these, respectively), we adopted a procedure expounded in Ref. [12] to obtain Gamow-Teller strength functions. We first used the Lanczos algorithm to obtain the lowest $3/2^-$ and $5/2^-$ states in ^{57}Fe to high precision. Next we created a ''collective'' $E2$ or $M1$ state by acting on the parent state with the relevant operator. We then used the collective state as the initial basis vector for an approximate Lanczos-based diagonalization of higher-lying states, yielding pseudoeigenvectors (PSEV's), which approximate the true states. We typically performed about 100 Lanczos iterations, resulting in about 100 PSEV's for each of the J_i's. In the Lanczos approach the lowest (and highest) several PSEV's are quite accurate representations of the corresponding eigenstates, while at intermediate energies the PSEV's converge more slowly, and after $\approx$100 iterations each still has contributions from tens to hundreds of actual eigenstates. It is easy to see, however, that all of the strength is contained in these PSEV's, which we used for the states nJ_i and nJ_f in Eq. (4). The wave functions used in each of the four terms in Eq. (4) were slightly different since they originated from different initial collective states.

So far we have not mentioned our choice of interaction. There are several effective interactions on the market, but (unfortunately) we did not know which was the best in this space. We were able to test the sensitivity of our results to the choice of Hamiltonian, however, and so used three different pf-shell interactions: the FPVH interaction of [13], the TBLC8 interaction of [14], and the FPBPN interaction (the FPD6 interaction of [15] with the single-particle energies modified to fit ^{56}Ni [16]). Each of these interactions reproduced the energy spectrum of low-lying states in ^{57}Fe reasonably well. The spread in the calculated values of the phase $\varepsilon_{E2}-\varepsilon_{M1}$ with these interactions provided a rough measure of theoretical uncertainty.

The last component of the calculation was the choice of effective $E2$ and $M1$ operators for each force. The matrix element $\langle 5/2||\ E2$ or $M1\ ||3/2\rangle$ normalizes each term in Eq. (4). Since the $M1$ matrix element [in the denominator in the second and fourth terms in Eq. (4)] is very small, it is particularly important, and we chose effective g values for the $M1$ operator in order to reproduce it accurately. Our prescription was to fix all of the $M1$ g values, except for the isoscalar spin piece ($g^s_{\rm IS}$), at their free nucleon values. For each interaction we then chose $g^s_{\rm IS}$ to give the correct matrix element for the first transition. The sign of the matrix element is not known, so we chose it consistently amongst the forces to obtain the most reasonable values for the set of $g^s_{\rm IS}$'s.

For the $E2$ operator a similar procedure gave unrealistic values for the effective charges e_p and e_n; we therefore adopted the ''canonical'' values $e_p=1.5e$ and $e_n=0.5e$ for all of the interactions. These values result in reasonable agreement with the first $E2$ matrix element, especially for the FPBPN force. In addition, the final phase ε_{E2} is only weakly dependent on the choice of the $E2$ effective charges. Table I summarizes the $E2$ and $M1$ matrix elements and total strengths for the few lowest states in both the large and small spaces. (The TBLC8 force shares a common heritage with the FPVH force and, since the results are similar, we omit TBLC8 from the tables.) In the large space the total strength for both multipoles is relatively insensitive to the force chosen. However, the $M1$ strength is about a factor of 10 larger than in the small space, dramatically illustrating the importance of including the $1f_{5/2}$ level.

How much did the nonconvergence of the intermediate PSEV's affect the results? The answer is very little for the $E2$ part of the phase, because the strength is concentrated at low energies and the energy denominator in Eq. (4) enhances the contribution of the low-lying converged states and reduces the effects of the higher-lying states. In Fig. 1 we show the distribution of $E2$ strength for the $3/2^-\rightarrow n(5/2)^-$ transitions (dashed line). It is completely dominated by transitions among the converged states. A similar result holds for the $E2$ in the $5/2^-\rightarrow n(3/2)^-$ direction. Though the effects of the energy denominator are also at work in the $M1$ piece of the phase, the distribution of $M1$ strength complicates

TABLE I. The absolute values of the $E2$ and $M1$ matrix elements for the FPVH and FPBPN forces compared to the experimentally determined values. The total calculated $E2$ and $M1$ strengths are also included.

Transition	Experiment	FPVH (small space)	FPVH (large space)	FPBPN (large space)
$M1\ \frac{5}{2})_1 \rightarrow \frac{3}{2})_1$	0.113	0.113	0.113	0.113
$E2\ \frac{5}{2})_1 \rightarrow \frac{3}{2})_1$	13.35	7.091	6.866	12.88
$M1\ \frac{5}{2})_2 \rightarrow \frac{3}{2})_1$	0.344	1.202	0.806	0.858
$E2\ \frac{5}{2})_2 \rightarrow \frac{3}{2})_1$	27.83	27.62	36.38	37.73
$M1\ \frac{3}{2})_2 \rightarrow \frac{5}{2})_1$	0.298	0.141	0.018	0.126
$E2\ \frac{3}{2})_2 \rightarrow \frac{5}{2})_1$	3.208	11.66	14.12	13.87
$B(M1)\ \frac{3}{2})_1 \rightarrow n\ \frac{5}{2}$		1.154	11.56	10.57
$B(E2)\ \frac{3}{2})_1 \rightarrow n\ \frac{5}{2}$		211.7	440.7	480.5
$B(M1)\ \frac{5}{2})_1 \rightarrow n\ \frac{3}{2}$		0.598	5.18	3.63
$B(E2)\ \frac{5}{2})_1 \rightarrow n\ \frac{3}{2}$		43.8	97.0	101.5.

matters. In Fig. 2 we show the total $M1$ strength for the $3/2^- \rightarrow n(5/2)^-$ transitions (dotted line); a broad resonance is visible at $\sim$12 MeV. Although this is the region where the PSEV's are unconverged, the $M1$ part of the phase nonetheless seems to be represented reasonably well. We make this statement after varying the number of Lanczos iterations and hence the number of PSEV's (converged and unconverged) to see if the phase changed appreciably as the approximations became more accurate. The size of the dependence is illustrated in Table II, where the $E2$ and $M1$ parts of the phase η (with $\overline{g_\rho}=1$) are listed for several numbers of iterations and for two different interactions. The $E2$ phases show essentially no dependence on the number of iterations (as implied above) and the $M1$ phases are not affected dramatically, indicating that the true result is not far from our best approximation.

The results in Table II allow us to constrain the parameter $\overline{g_\rho}$ and estimate the uncertainty. The FPVH and the FPBPN forces give very similar results for each piece of the phase and the final phases are very close. The TBCL8 interaction gives a similar result, $\varepsilon_{E2}-\varepsilon_{M1}=-24.2\times10^{-3}$. The lack of dependence on the interaction suggests that the uncertainty in the results is not large. Table II also suggests that the phase is insensitive to the size of the model space, but this turns out to be a coincidence. In the small space, all of the $M1$ piece of the phase lies at very low excitation energy, mirroring the initial upward peak at 2–3 MeV in Fig. 2. But the fall in the phase from 3–10 MeV and the subsequent rise due to the $M1$ resonance are not present in the small space and so the agreement on the final value of ε_{M1} between the two model spaces is accidental.

The entries in Table II were evaluated with $\overline{g_\rho}=1$. Neglecting theoretical error, which we have argued should be fairly small, and averaging the results from the FPVH and FPBPN forces in the large space, we conclude that $|\varepsilon_{E2}-\varepsilon_{M1}|/\overline{g_\rho}=16.4\times10^{-3}$. The experimental value for

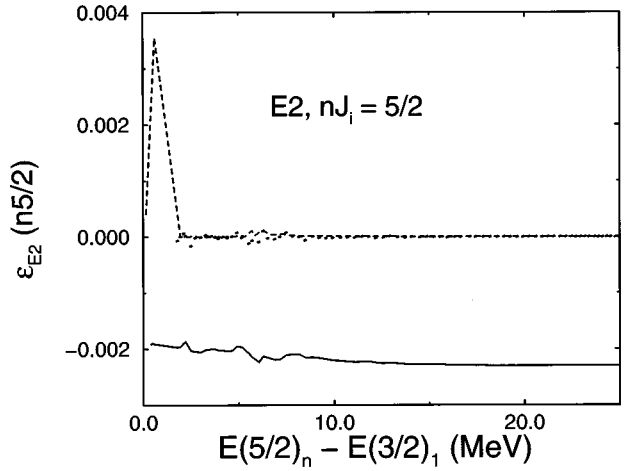

FIG. 1. The piece of ε_{E2} arising from $E2$ transitions with $J_f=3/2 \leftarrow nJ_i=5/2$ using the FPBPN force in the large space. The solid line is the sum from Eq. (4). The points correspond to the individual points in the sum. The dashed line is the individual $B(E2)$ in $e^2\,\mathrm{fm}^4$ divided by a factor of 10^5. It is apparent that ε_{E2} is well converged at low excitation energies.

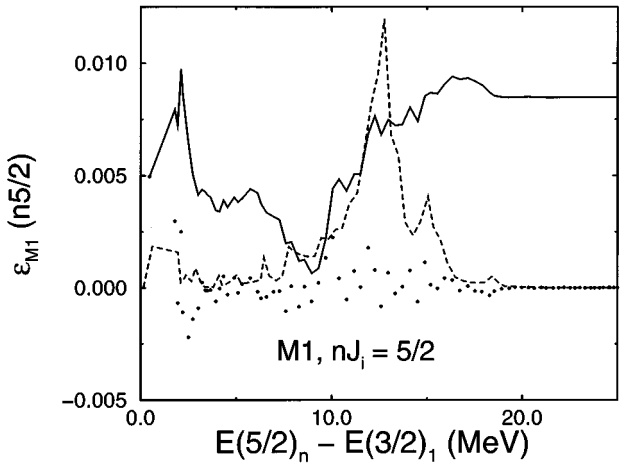

FIG. 2. The piece of ε_{M1} arising from $M1$ transitions with $J_f=3/2 \leftarrow nJ_i=5/2$ using the FPBPN force in the large space. The solid line is the sum from Eq. (4). The points correspond to the individual points in the sum. The dashed line is the individual $B(M1)$ in nuclear magnetons divided by a factor of 100. ε_{M1} is well converged at excitation energies above 20 MeV.

TABLE II. The phases, with $\overline{g_\rho}=1$ in Eq. (5) and multiplied by a factor of 10^3, computed with the FPVH and FPBPN interactions. The number of Lanczos iterations is listed to illustrate the convergence of the phases. 200 iterations were performed only for the cases listed. Each of columns 3–6 corresponds to one of the terms in Eq. (4); for example, the heading $\varepsilon_{E2}(n3/2)$ corresponds to the first term of the equation with $J_i=5/2$ and $nJ_f=3/2$. The last column contains the final phase calculated according to Eq. (4).

Force (space)	Lanczos iterations	$\varepsilon_{E2}(n3/2)$	$\varepsilon_{E2}(n5/2)$	$\varepsilon_{M1}(n3/2)$	$\varepsilon_{M1}(n5/2)$	$\varepsilon_{E2}-\varepsilon_{M1}$
FPVH (small)	Complete	-5.08	-5.15	7.04	10.10	-27.6
FPBPN (small)	Complete	-6.50	-5.84	7.94	13.03	-33.3
FPVH (large)	100	-3.239	-2.322	-0.814	12.681	-17.4
FPVH (large)	200	-3.239		-0.691		
FPBPN (large)	60	-2.436	-2.306	1.913	8.5052	-15.2
FPBPN (large)	100	-2.425	-2.298	2.135	8.4813	-15.3
FPBPN (large)	200			1.769		

$|\sin\eta|$, Eq. (2), then implies that

$$|\overline{g_\rho}|=(2\pm4)\times10^{-2}. \tag{6}$$

This number is comparable to the best limits from other experiments. Limits on electric dipole moments, for example, correspond to $|\overline{g_\rho}|\lesssim10^{-2}$, and the new data on neutron-holmium [17] scattering yields $|\overline{g_\rho}|=(2.3\pm2.1)10^{-2}$. Perhaps coincidentally, all these very different experiments give roughly the same limit. It has been suggested [18], however, that upcoming detailed balance experiments, which go through complicated compound nuclear states, may provide limits that are better than these by 2 orders of magnitude. Even though recent theoretical work [19,20] indicates that one cannot expect $\overline{g_\rho}$ to be much larger than 10^{-8}, it remains worthwhile to translate limits from other experiments into limits on $\overline{g_\rho}$. Theoretical expectations are easily and often confounded, and it is important to know which of the many experiments reported in the literature (and still to come) have the best chance of actually seeing time reversal violation.

We thank David Resler for several helpful discussions and help with the modifications to the code CRUNCHER. This work was supported in part by the U.S. Department of Energy under Grants DE-FG05-94ER40827 and DE-FG03-88ER-40397 and by the U.S. National Science Foundation under Grants PHY94-12818 and PHY94-20470. M.T.R. is supported by the Weingart Foundation. Part of the computing was carried out at Lawrence Livermore National Laboratory, operated under the auspices of the U.S. Department of Energy under Grant W-7405-ENG-48.

[1] W.C. Haxton, A. Höring, and M. Musolf, Phys. Rev. D **50**, 3422 (1994).
[2] M. Simonius, Phys. Lett. **58B**, 147 (1975).
[3] J. Engel, C.R. Gould, and V. Hnizdo, Phys. Rev. Lett. **73**, 3508 (1994).
[4] E. Blanke *et al.*, Phys. Rev. Lett. **51**, 355 (1983).
[5] N.K. Cheung, H.E. Henrikson, and F. Boehm, Phys. Rev. C **16**, 2381 (1977).
[6] M. Beyer, Phys. Rev. C **48**, 906 (1993); Nucl. Phys. **A493**, 335 (1989).
[7] E.M. Henley and B.A. Jacobson, Phys. Rev. **113**, 225 (1959); E.M Henley, Annu. Rev. Nucl. Part. Sci. **19**, 367 (1969).
[8] L.C. Beidenharn and M.E. Rose, Rev. Mod. Phys. **25**, 729 (1953).
[9] B.R. Davis, S.E. Koonin, and P. Vogel, Phys. Rev. C **22**, 1233 (1980).
[10] R.J. Blin-Stoyle and F.A. Bezerra Coutinho, Nucl. Phys. **A211**, 157 (1973).
[11] D.A. Resler and S.M. Grimes, Comput. Phys. **2**, 65 (1988).
[12] S.D. Bloom and G.M. Fuller, Nucl Phys. **A440**, 511 (1985); G.J. Mathews *et al.*, Phys. Rev. C **32**, 796 (1985).
[13] A. van Hees and P. Glaudemans, Z. Phys. A **303**, 267 (1981); J. van Heinen, W. Chung, and B.H. Wildenthal, *ibid.* **269**, 159 (1976).
[14] M.G. van der Merwe, W.A. Richter, and B.A. Brown, Nucl. Phys. **A579**, 173 (1994).
[15] W.A. Richter, M.G. van der Merwe, R.E. Julies, and B.A. Brown, Nucl. Phys. **A523**, 325, (1991).
[16] B.A. Brown (private communication).
[17] C. Gould (private communication).
[18] O.K. Vorov, Phys. Lett. B **368**, 301 (1996).
[19] Jonathan Engel, Paul H. Frampton, and Roxanne P. Springer, Phys. Rev. D **53**, 5112 (1996).
[20] R.S. Conti and I.B. Khriplovich, Phys. Rev. Lett. **68**, 3262 (1992).